Strongly peraluminous granites provide independent evidence for an increase in biomass burial across the Precambrian-Phanerozoic boundary

Sami Mikhail[1*], Eva E. Stüeken[1], Toby J. Boocock[1], Megan Athey[1], Nick Mappin[1], Adrian J. Boyce[2], Janne Liebmann[3], Christopher J. Spencer[4], Claire E. Bucholz[5]

[1]*School of Earth & Environmental Sciences, University of St Andrews, KY16 9TS, UK*

[2]*Scottish Universities Environmental Research Centre, East Kilbride, G75 0QF, UK*

[3]*Timescales of Mineral Systems Group, School of Earth and Planetary Sciences, Curtin University, Perth, Western Australia 6102, Australia*

[4]*Department of Geological Sciences and Geological Engineering, Queens University, Ontario, K7L 3N6, Canada*

[5]*Division of Geological and Planetary Sciences, California Institute of Technology, Pasadena, California 91125, USA*

*Corresponding Author: sm342@st-andrews.ac.uk

ABSTRACT

Strongly peraluminous granites (SPGs) are generated by the partial melting of sedimentary rocks and can thus provide a novel archive to reveal secular trends in Earth's environmental history that integrate siliciclastic sedimentary lithologies. The nitrogen (N) content of Archean, Proterozoic, and Phanerozoic SPGs reveals a systematic increase across the Precambrian-Phanerozoic boundary. This rise is supported by a coeval increase in the phosphorus (P) contents of SPGs. Collectively, these data are most parsimoniously explained by an absolute increase in biomass burial in the late Proterozoic or early Phanerozoic by a factor of approximately 5 and up to 8. The Precambrian-Phanerozoic transition was a time of progressive oxygenation of surface environments paired with major biological innovations, including the rise of eukaryotic algae to ecological dominance. Because oxygenation suppresses biomass preservation in sediments, the increase in net biomass burial preserved in SPGs reveals an expansion of the biosphere and an increase in primary production across this interval.

INTRODUCTION

Quantifying changes in biomass burial through time has occupied scientists for decades because organic carbon is a strong reductant, and so biomass burial constitutes an indirect source of O_2 that may have driven atmospheric oxygenation (e.g., Canfield, 2021; Wickman, 1956). Recent studies have relied on complex biogeochemical models to calculate trends in biomass burial over time (Planavsky et al., 2022; Krissansen-Totton et al. 2021). While such models advance our mechanistic understanding of paleoenvironmental conditions, their results disagree, and they imply that rates of biomass burial cannot easily be read from the carbon isotope record as was originally envisioned (e.g., Des Marais et al., 1992). Therefore, new empirical approaches are required to provide independent constraints on secular shifts in biomass burial. Some advances have been made with the record of diamictites, which preserve evidence of increased biomass storage in continental crust across the Precambrian-Phanerozoic transition (Johnson and Goldblatt, 2017; Han et al., 2023); however, this approach is limited by the sparse preservation of diamictites in the geological record.

We leverage the record of nitrogen (N) in strongly peraluminous granites (SPGs) as an indirect archive of biomass buried in sediments through time. Strongly peraluminous

granites (SPGs) are defined as granites with an aluminum saturation index ASI = molar $Al_2O_3/(CaO+Na_2O+K_2O)$] > 1.1 and dominantly formed via the partial melting of sedimentary rocks (e.g., Clarke, 2019; Nabelek, 2020; Bucholz, 2023). Crucially, SPGs integrate large volumes of terrigenous siliciclastic sediments deposited in marine settings through anatexis (most commonly in collisional to post-collisional orogens) and have been shown to record geochemical information about their sedimentary protoliths (e.g., Bucholz et al., 2020; Liebmann et al., 2021). Our approach contrasts with studies of total organic carbon (TOC) and N in sedimentary archives, which emphasize organic-rich shales (Ader et al. 2016). Carbonaceous compounds (CO_3^{2-}, CO_2, CH_4) are devolatilized and lost from the system during sediment melting (anatexis) and igneous differentiation because they do not partition into granite-forming minerals. Nitrogen and P, however, can be retained by crystalising mineral phases with NH_4^+ substituting for K^+ and/or Rb^+ (Boocock et al., 2023a) and P being retained by apatite and monazite (Bea, 1996).

METHODS

Analytical Geochemistry

The samples analyzed in this study span a large range of formation ages (2700-21 Ma), provenances, and tectonic settings (see supplementary dataset). Nitrogen abundances and isotope values were obtained from whole rock powders using sealed tube combustion followed by gas-source IRMS at the University of St Andrews (Boocock et al., 2020). Major and trace element data were collated from the literature or obtained via energy-dispersive X-ray fluorescence at the University of St Andrews. Oxygen isotope data were obtained by laser fluorination IRMS at the Scottish Universities Environmental Research Centre (SUERC) (full analytical details are provided in the Supplemental Methods).

Filtering the Nitrogen database

To complement our sample suite, we compiled data for igneous rocks from the literature (see Supplementary Dataset). Results reported as ug/g NH_4^+ were converted to ug/g N. We filtered for granitic rocks, either geochemically (SiO_2 > 67 wt.%) or mineralogically (i.e., QAPF), and extracted those data from granites which are strongly peraluminous, either geochemically (where the ASI is published and ≥ 1.1; n = 24) or where they host primary peraluminous minerals (i.e., biotite + muscovite, cordierite, and garnet; n = 37). Altered samples, as identified by the original authors, were removed from the compilation.

RESULTS

N concentrations for SPGs are lower in the Archean (3-23 µg/g, mean = 8 ± 5 µg/g) and Proterozoic (4-15 µg/g, mean = 9 ± 4 µg/g) compared to the Phanerozoic (2-189 µg/g, mean = 76 ± 54 µg/g) (Table 1). The difference between the Archean and Proterozoic is statistically insignificant ($p = 0.5$), but the difference between the Precambrian and the Phanerozoic is significant ($p < 10^{-13}$). Nitrogen isotope values ($\delta^{15}N$) for SPGs, where available, are indistinguishable between the Archean (mean +5.5 ± 3.6 ‰) and Proterozoic (mean +4.7 ± 2.0 ‰), but show a significant ($p = 10^{-3}$) increase towards the Phanerozoic (mean +7.9 ± 1.8 ‰; Table 1).

DISCUSSION

The origin of nitrogen in SPGs

To ensure robustness of our approach, we first need to evaluate whether SPGs primarily record the geochemistry of their sedimentary protoliths and are free from significant alteration. In extrusive igneous rocks, it has been demonstrated that nitrogen can become enriched through progressive magmatic differentiation of an initially N-poor melt, behaving similarly to Large Ion Lithophile Elements (LILE; Boocock et al., 2023b). However, in this sample set, we find no co-variation for [N] or $\delta^{15}N$ versus any index of petrological evolution, such as SiO_2 vs. K_2O (Fig.1), Rb, and K/Rb, or relative to the abundances of mafic elements ($FeO+MgO+TiO_2$; R^2 = 0.17, 0.10, and 0.23, respectively). Further, as K-bearing phases are the dominant host of nitrogen in igneous rocks (Hall, 1999; Boocock et al., 2023a), the lack of a linear relationship between N and K_2O suggests that the

abundance of potassic phases in the samples is not controlling their N budget. Therefore, the N concentration of SPGs either reflects protolith geochemistry or post-emplacement alteration. We observe no correlation between either [N] or $\delta^{15}N$ against proxies for post-emplacement alteration, such as the loss on ignition (R^2 = 0.0056 and 0.0093, respectively) or bulk rock $\delta^{18}O$ values (R^2 = 0.09 and 0.009, respectively). We note that only limited LOI and $\delta^{18}O$ data are available for the Phanerozoic SPGs; however, it is unlikely that fluid alteration would have increased systematically from Precambrian into the Phanerozoic and affected N and P simultaneously. Thus, we find no evidence to suggests that fluid alteration was the dominant source of N for the N-rich SPGs, which are primarily Phanerozoic. The similarity in [N] and $\delta^{15}N$ between Proterozoic and Archean SPGs suggests that both sample suites preserve the same information about the N geochemistry of their sedimentary protolith, and therefore, the N enrichment observed for Phanerozoic SPGs likely reflects a greater N endowment in the source of Phanerozoic SPGs.

The N:P of SPGs are unlikely equal to the N:P of the metasedimentary source(s) because the uptake of both elements during SPG formation are controlled by different phase equilibria. The N content of SPGs is affected by devolatilization during diagenesis and metamorphism, and the extent of this can vary over an order of magnitude from nearly full retention to >80% loss (Busigny et al. 2003; Haendel et al., 1986; Jia et al., 2006; Palya et al., 2011), whereas data for the leucosome and melanosome portions from the Pefia Negra migmatite complex show that anatectic melts are N-depleted relative to the mica-feldspar bearing restite (D = 0.5 ± 0.1; Hall et al., 1996). Experimental data show that when present in trace quantities (ca. < 2500 ug/g) N partitions into K-bearing minerals over fluids and reaches parity for melts vs fluids (with a $D_{N\ melt\text{-}fluid}$ ca. 1; Jackson and Cottrell, 2023). Hence, changes in the primary N content of SPGs should reflect – but underestimate – the relative N abundances of (meta-)sedimentary sources. Herein we assume that the underestimation (fraction of N retained during metamorphism and anatexis) is uniform through time, and therefore secular trends observed in N geochemistry of SPGs averaged over several plutons reflect relative changes in sediment composition. This argument is consistent with the observation that the median N contents of strongly peraluminous granites are higher than metaluminous granites (ASI < 1; Hall, 1999). The P content of SPGs is not affected by devolatilization but is fractionated during anatexis. The P concentration in the anatectic melt is controlled dominantly by apatite breakdown, which is a complex function of initial P concentration of the sedimentary source, apatite solubility in the melt as a function of temperature and pressure, the extent of melting, and the ability of apatite to be in equilibrium with the melt (e.g., whether it is included in another phase; Yakymchuk, 2017; Bucholz, 2022). Further, after extraction of the melt from the source, P concentrations in the granitic melt evolve with differentiation. However, after accounting for all these processes in detail, an increase from an average sedimentary P_2O_5 concentration of ~0.1 wt.% prior to ~720 Ma to 0.5 wt.% after 720 Ma (Reinhard et al., 2017) can explain a corresponding increase in average SPG P_2O_5 concentrations from 0.11 to 0.24 wt.% (Bucholz, 2022). Thus, an increase by a factor of 2.2 in average SPG concentrations across this time interval broadly agrees with an increase in a factor of 5 in average sedimentary P_2O_5 concentration. Ergo, while we acknowledge that the major and trace element geochemistry of SPGs will not directly mirror their source, nor will the source of any two SPGs mirror one and other, the dominant controlling factor for N and P geochemistry in SPGs is their source composition, which dominated by (meta-)sedimentary siliciclastic lithologies (Clarke, 2019; Nabelek, 2020; Bucholz, 2023).

Increasing biomass burial across the Precambrian-Phanerozoic boundary

The average N and P concentrations in Phanerozoic SPGs rise by factors of 8.4 and 2.2, respectively (Figure 2). This trend is mirrored by data from glacial diamictites, which show an increase in the relative concentrations of N (Johnson and Goldblatt, 2017) and fluorine (Han et al., 2023) after the Proterozoic. The absence of N data between 470-1435 Ma means that we cannot resolve the rate of the N increase(s) (Fig.2), however, the P record is more complete and suggests that this occurred between 800-500 Ma (Figure 2c). We

stress that the sedimentary protoliths of SPGs may pre-date SPGs by millions of years and this prohibits a direct determination for timing. Furthermore, non-sedimentary crustal rocks likely contribute to SPG formation. However, our data unequivocally show a 5-to-8-fold increase in the N and P abundances in Phanerozoic SPGs relative to Precambrian SPGs (Fig.2). We rule out a shift in tectonic style to explain this increase because continental shelves as the major loci of biomass burial have existed since continental emergence in the Neoarchean (Flament et al. 2008). Archean shales with organic carbon abundances like the Neogene support this idea (Lyons et al. 2014). Furthermore, by taking secular averages, our results integrate over SPGs formed in a variety of tectonic regimes such as arc-continent (i.e. Scotland) or continent-continent orogenies (i.e., Himalayas). Also changes in mantle temperature, pressure, fluids, and oxygen fugacity can be ruled out as explanations (see supplements). Thus, the most likely explanation for our data is an increase in the amount of biomass in sediments.

Converting the N and P factor increases to absolute sedimentary-hosted biomass is difficult for the reasons noted above, but also because the C:N:P of biomass may have changed over time (Planavsky, 2014). Moreover, the sedimentary input for SPGs is likely a combination of terrigenous and marine. There is no simple factor to convert [N] or [P] of SPG into carbon contents of sediments. If we assume, however, that the global average C:N:P of biomass has not changed systematically, our results suggest that total biomass burial would have increased by a factor of 5 to 8 across the Precambrian-Cambrian boundary, and we can compare our observations to previous predictions. Krissansen-Totton et al. (2021) modelled the carbon cycle benchmarked to $^{13}C/^{12}C$ to investigate biomass burial relative to total C deposition (f_{org}) since 4 Ga. Their model suggested that f_{org} increased by a factor of 2-5 from the Archean to the modern while absolute biomass burial remained constant (within error). By contrast, Planavsky et al. (2022) derived an overall increase in f_{org} and absolute biomass burial by factors of >10. Our results provide a new independent constraint for biomass burial that falls in between these modelled estimates (5-to-8). Our data indicate that this shift manifests in the Phanerozoic and may be linked to the rise of macro-organisms, which may have created ballast and facilitated settling of organic matter on the seafloor (Logan et al., 1995).

Our N isotope data can speak to shifts in the supply of fixed nitrogen to the biosphere, akin to the use of $\delta^{15}N$ in sedimentary rocks (Ader et al., 2016). It is likely that N isotopes undergo fractionation during sediment melting, as it has been documented that $\delta^{15}N$ increases with regional metamorphism (by ~ +6 ‰; e.g., Haendel et al., 1986). However, since all SPGs are derived from metasedimentary rocks that have experienced high grade metamorphism (T > 680 ºC), the fractionation of N isotopes during metamorphism should be similar and independent of time. Thus, it suggests that Phanerozoic sediments displayed on average higher $\delta^{15}N$ values compared to the Precambrian (Table 1). This may be consistent with a larger reservoir of nitrate in Phanerozoic seawater, which was partly assimilated into biomass and buried in sediments (Ader et al., 2016). The secular shift in $\delta^{15}N$ values seen in SPGs, which integrate over all sediment types, is in fact more in line with other proxies indicating ocean oxygenation in the Neoproterozoic or early Palaeozoic (Wei et al. 2021). Nitrate is most stable under oxic conditions and constitutes the major N source for eukaryotic algae (Anbar and Knoll, 2002). The Precambrian-Phanerozoic transition was a time of progressive oxygenation of surface environments paired with major biological innovations, including the rise of eukaryotic algae to ecological dominance (Brocks et al., 2017). Oxygenation would have suppressed biomass preservation in sediments (Kipp et al. 2021), and therefore an increase in net biomass burial at this time implies an expansion of the biosphere and an increase in primary production. This transition was likely supported by greater nutrient availability (as supported by N isotopic data), and it may have contributed to long-term atmospheric evolution.

CONCLUSIONS

SPGs preserve relative changes in sedimentary geochemistry through time. Nitrogen concentrations in SPGs require a significant increase in the average N content of sediments by a factor of 8.4 from the Precambrian to the Phanerozoic, accompanied by a corresponding increase in sedimentary P by a factor of ~5 across the same time interval. The P record suggests this transition happened between 800-500 Ma (Fig.2). Notably, both N and P are major constituents of biomass and their concurrent increase in SPGs is most parsimoniously explained by enhanced biomass burial in sediments around the world at that time. These results provide a new empirical anchor point for reconstructing the evolution of life and understanding the interaction between the biosphere, atmosphere, and magmatic systems of Earth.

ACKNOWLEDGEMENTS

Funding was provided by a Natural Environment Research Council (NERC) studentship (NE/R012253/1) to TJB and a National Environmental Isotope Facility access grant (NEIF – 2313.0920) to EES, SM and TJB. SM was supported by NERC (NE/PO12167/1). EES was supported by NERC (NE/V010824/1). We thank Alison MacDonald at SUERC for oxygen isotope support. We thank Charlotte Gordon, Roberto Weinberg, Mike Searle, and Kathryn Coffey for sample provisions.

Figure 1. Whole-rock (WR) nitrogen concentrations for SPGs vs [a] SiO_2 and [b] K_2O. Note the lack of trends for [N] versus two indices of petrological evolution. Uncertainties are smaller than the symbol size.

Figure 2. SPG whole-rock N [a-b] and P [c-d] data through time. The P data are locality averages (not individual analyses), see Bucholz (2022) for compilation. The P data for Phanerozoic SPGs are selected for samples where the photolith was known to be < 720 Ma (Bucholz, 2022). The full dataset (and sources) is provided in the supplementary material. Uncertainties on measured N contents are < 10%. There is no x-axis scaling for b and d.

Table 1. Means and medians for key geochemical variables.

CONTRIBUTIONS:

EES and SM conceived the project; CEB, JL and CS provided samples and auxiliary data; TJB, MA and NM performed geochemical analyses at St Andrews; TJB and AB collected the oxygen isotope data. SM and EES wrote the manuscript with contributions from all authors.

REFERENCES

Ader, M., Thomazo, C., Sansjofre, P., Busigny, V., Papineau, D., Laffont, R., Cartigny, P., Halverson, G.P., 2016. Interpretation of the nitrogen isotopic composition of Precambrian sedimentary rocks: Assumptions and perspectives. Chem. Geol. 429, 93–110.

Anbar, A.D. Knoll, A.H., 2002. Proterozoic ocean chemistry and evolution: a bioinorganic bridge? Science, 297, 1137-1142.

Bea, F. 1996. Residence of REE, Y, Th and U in granites and crustal protoliths; implications for the chemistry of crustal melts. J. Petrol. 57, 521–552.

Boocock, T.J., Mikhail, S., Prytulak, J., Di Rocco, T., Stüeken, E.E., 2020. Nitrogen Mass Fraction and Stable Isotope Ratios for Fourteen Geological Reference Materials: Evaluating the Applicability of Elemental Analyser Versus Sealed Tube Combustion Methods. Geostand. Geoanalytical Res. 44, 537–551.

Boocock, TJ., Mikhail, S., Stüeken, ES., Bybee, GM., König, R., Boyce, AJ., Prytulak, J., Buisman, I. 2023a. Equilibrium partitioning and isotopic fractionation of nitrogen between

biotite, plagioclase, and K-feldspar during magmatic differentiation. Geochimica et Cosmochimica Acta. 356, 116-128

Boocock, TJ., Mikhail, S., Boyce, AJ., Prytulak, J., Savage, PS., Stüeken, ES. 2023b. A primary magmatic source of nitrogen to the Earth's crust. Nature Geoscience. 16, 521–526.

Brocks, J.J., Jarrett, A.J., Sirantoine, E., Hallmann, C., Hoshino, Y. Liyanage, T. 2017. The rise of algae in Cryogenian oceans and the emergence of animals. Nature, 548, 578-581.

Bucholz, C.E., Spencer, C.J., 2019. Strongly Peraluminous Granites across the Archean–Proterozoic Transition. J. Petrol. 60, 1299–1348.

Bucholz, C.E., Biasi, J.A., Beaudry, P., Ono, S. 2020. Sulfur isotope behavior during metamorphism and anatexis of Archean sedimentary rocks: A case study from the Ghost Lake batholith, Ontario, Canada. Earth and Planetary Science Letters. 549, 116494.

Bucholz, C.E., 2022. Coevolution of sedimentary and strongly peraluminous granite phosphorus records. Earth Planet. Sci. Lett. 596, 117795.

Bucholz, C.E., 2023. The diversity and origin of granites. Treatise on Geochemistry (Third Edition). *In Press*.

Canfield, D.E. 2021. Carbon cycle evolution before and after the great oxidation of the atmosphere. Amer. J. Sci. 321, 297–331.

Clarke, D.B. 2019. The origins of strongly peraluminous granitoid rocks. The Canadian Mineralogist. 57, 529-550.

Flament, N., Coltice, N. and Rey, P.F. 2008. A case for late-Archaean continental emergence from thermal evolution models and hypsometry. Earth and Planetary Science Letters. 275, 326-336.

Haendel, D., Mühle, K., Nitzsche, H.M., Stiehl, G. Wand, U., 1986. Isotopic variations of the fixed nitrogen in metamorphic rocks. Geochim. Cosmochim. Acta. 50, 749-758.

Hall, A. 1999. Ammonium in granites and its petrogenetic significance. Earth Sci. Rev. 45, 145–165.

Hall, A., Periera, M.D., Bea, F. 1996. The abundance of ammonium in the granites of central Spain, and the behaviour of the ammonium ion during anatexis and fractional crystallization. Mineral. Petrol. 56, 105–123.

Han, P-H., Rudnick, R.L., He, T., Marks, M.A.W., Wang, S-J., Gaschnig, R., Hub, Z-C. 2023. Halogen (F, Cl, Br, and I) concentrations of the upper continental crust through time as recorded in ancient glacial diamictite composites. Geochim. Cosmochim. Acta. 341, 28-45.

Jackson, C.R.M., Cottrell, E. 2023. Nitrogen partitioning between silicate phases and aqueous fluid depends on concentration. Geochim. Cosmochim. Acta. 354, 1-12.

Jia, Y. 2006. Nitrogen isotope fractionations during progressive metamorphism: A case study from the Paleozoic Cooma metasedimentary complex, southeastern Australia. Geochim. Cosmochim. Acta. 70, 5201-5214.

Johnson, B.W., Goldblatt, C., 2017. A secular increase in continental crust nitrogen during the Precambrian. Geochemical Perspect. Lett. 24–28.

Krissansen-Totton, J., Kipp, M.A. and Catling, D.C., 2021. Carbon cycle inverse modeling suggests large changes in fractional organic burial are consistent with the carbon isotope record and may have contributed to the rise of oxygen. Geobiology, 19(4), pp.342-363.

Kipp, M.A., Krissansen-Totton, J. Catling, D.C. 2021. High organic burial efficiency is required to explain mass balance in Earth's early carbon cycle. *Global Biogeochemical Cycles*, *35*.

Liebmann, J., Spencer, C.J., Kirkland, C.L., Bucholz, C.E., Xia, X.P., Martin, L., Kitchen, N., Shumlyanskyy, L., 2021. Coupling sulfur and oxygen isotope ratios in sediment melts across the Archean-Proterozoic transition. Geochimica et Cosmochimica Acta, 307, pp.242-257.

Logan, G.A., Hayes, J.M., Hieshima, G.B., Summons, R.E. 1995. Terminal Proterozoic reorganization of biogeochemical cycles. Nature. 376, 53-56.

Lyons, T.W., Reinhard, C.T., Planavsky, N.J. 2014. The rise of oxygen in Earth's early ocean and atmosphere. Nature. 506, 307–15.

Nabelek, P.I. 2020. Petrogenesis of leucogranites in collisional orogens. Geological Society, London, Special Publications. 491, 179-207.

Palya, A.P., Buick, I.S., Bebout, G.E., 2011. Storage and mobility of nitrogen in the continental crust: Evidence from partially melted metasedimentary rocks, Mt. Stafford, Australia. Chem. Geol. 281, 211–226.

Planavsky, N.J., Fakhraee, M., Bolton, E.W., Reinhard, C.T., Isson, T.T., Zhang, S., Mills, B.J., 2022. On carbon burial and net primary production through Earth's history. American Journal of Science, 322(3), pp.413-460.

Planavsky, N.J., 2014. The elements of marine life. Nature Geoscience. *7*, 855-856.

Reinhard, C.T., Planavsky, N.J., Gill, B.C., Ozaki, K., Robbins, L.J., Lyons, T.W., Fischer, W.W., Wang, C., Cole, D.B., Konhauser, K.O. 2017. Evolution of the global phosphorus cycle. Nature. 541, 386–389.

Wei, G.Y., Planavsky, N.J., He, T., Zhang, F., Stockey, R.G., Cole, D.B., Lin, Y.B. Ling, H.F. 2021. Global marine redox evolution from the late Neoproterozoic to the early Paleozoic constrained by the integration of Mo and U isotope records. *Earth-Science Reviews*, *214*, 103506.

Wickman, F.E., 1956. The cycle of carbon and the stable carbon isotopes. Geochimica et Cosmochimica Acta. 3, 136-153.

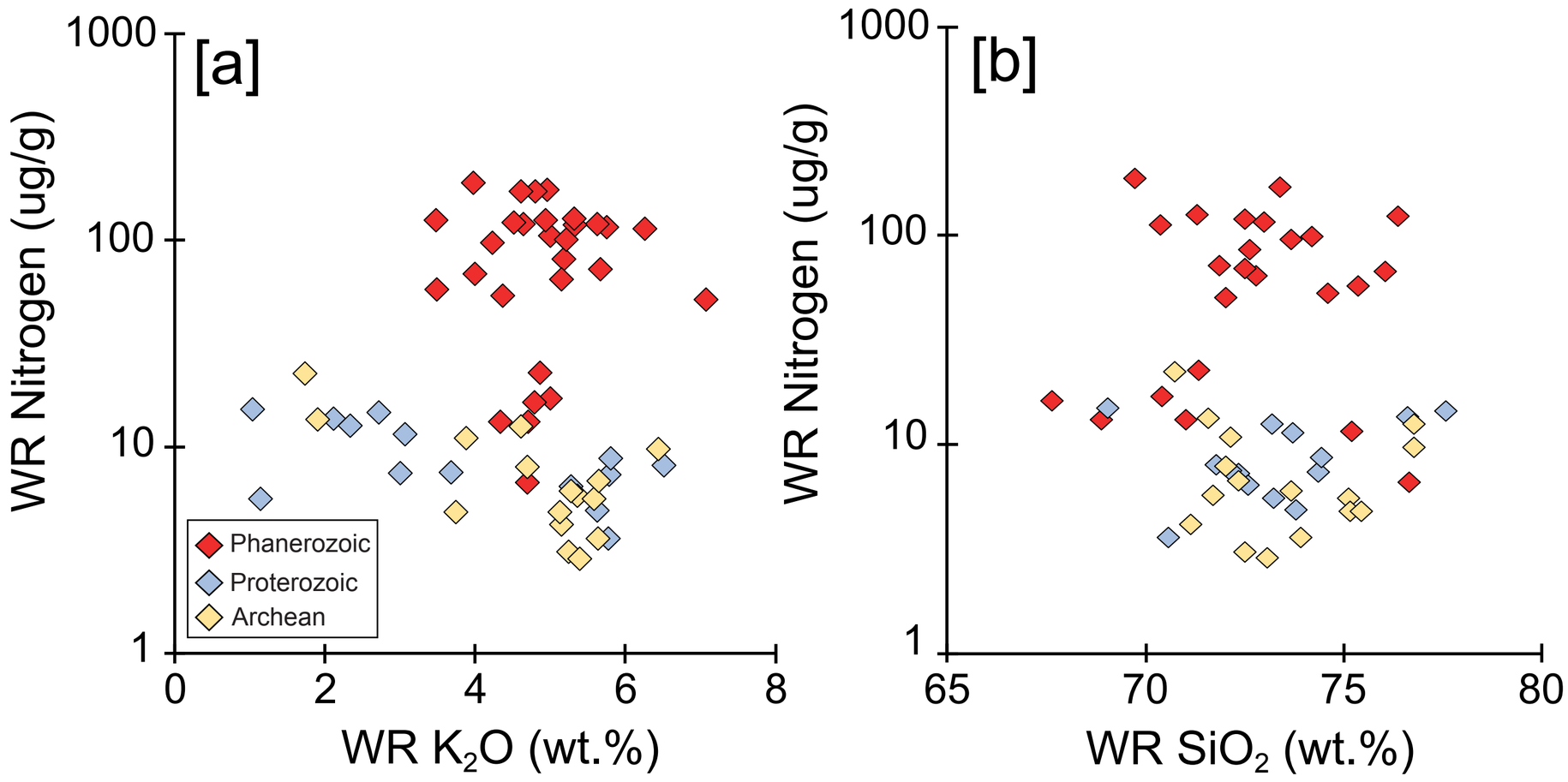
[a]
[b]
1000
100
10
1
WR Nitrogen (ug/g)
0
2
4
6
8
WR K2O (wt.%)
65
70
75
80
WR SiO2 (wt.%)
Phanerozoic
Proterozoic
Archean

Figure 1

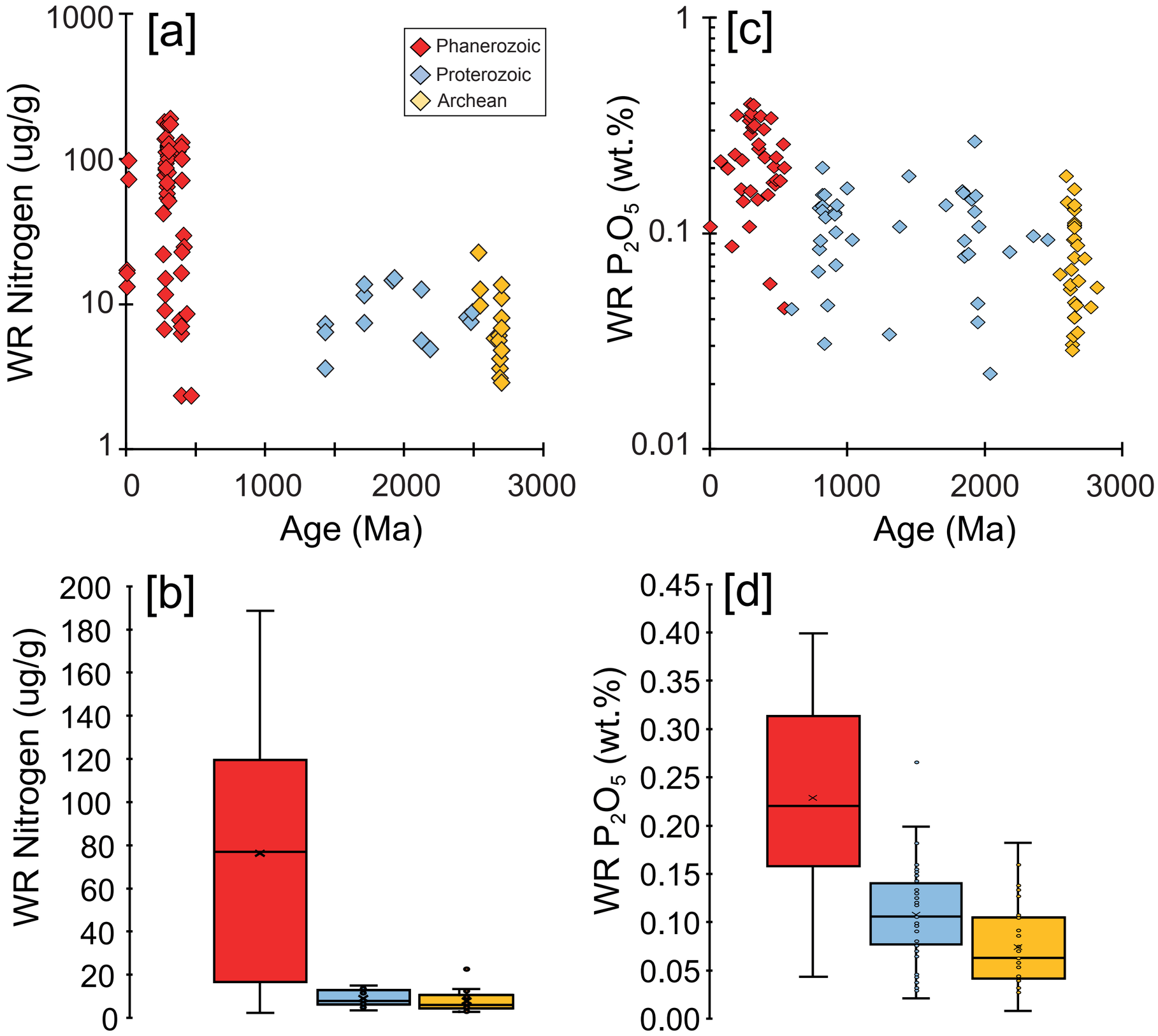
[a]
Phanerozoic
Proterozoic
Archean
WR Nitrogen (ug/g)
1000
100
10
1
0
1000
2000
3000
Age (Ma)
[c]
WR P_2O_5 (wt.%)
1
0.1
0.01
0
1000
2000
3000
Age (Ma)
[b]
WR Nitrogen (ug/g)
200
180
160
140
120
100
80
60
40
20
0
[d]
WR P_2O_5 (wt.%)
0.45
0.40
0.35
0.30
0.25
0.20
0.15
0.10
0.05
0.00

Figure 2

		Archean	Proterozoic	Phanerozoic
ASI	Mean	1.2	1.4	1.3
	StDev	0.1	0.2	0.1
[N]	Mean	8	9	76
µg/g	Median	6	8	77
	StDev	5	4	54
	n	16	14	61
$\delta^{15}N$	Mean	5.5	4.7	7.9
‰	Median	5.2	4.2	8.4
	StDev	3.6	2	1.8
	n	16	13	15
$\delta^{18}O$	Mean	9.1	10.2	10
‰	Median	9.3	10.8	9.7
	StDev	0.6	1.8	0.7
	n	9	9	5
N/ASI	Mean	6	9	39
	Median	3	8	31
	StDev	8	4	32
N/K	Mean	6	7	58
	Median	5	6	59
	StDev	4	2	40
K_2O	Mean	4.7	3.8	4.8
wt.%	Median	5.2	3.4	4.7
	StDev	1.3	1.9	0.9
SiO_2	Mean	73.4	73.2	72.6
wt.%	Median	72.8	73.2	72.6
	StDev	2	2.2	2.4

Table 1